

Spin Transfer Torques by Point-Contact Spin Injection

T. Y. Chen¹, Y. Ji², S. X. Huang¹, and C. L. Chien¹, M. D. Stiles³

¹*Department of physics and astronomy, The Johns Hopkins University, Baltimore, MD 21218*

²*Department of Physics and Astronomy, University of Delaware, Newark, DE 19716*

³*National Institute of Standards and Technology, Gaithersburg, MD 20899*

Abstract

Spin-transfer torques (STT) provides a new mechanism to alter the magnetic configurations in magnetic heterostructures, a feat previously only achieved by an external magnetic field. A current flowing perpendicular through a magnetic noncollinear spin structure can induce torques on the magnetization, depending on the polarity of the current. This is because an electron carries angular momentum, or spin, part of which can be transferred to the magnetic layer as a torque. A spin-polarized current of a substantial current density (e.g., 10^8 A/cm²) is required to observe the effect of the spin transfer torques. Consequently, switching by spin-polarized currents is often realized in small structures with sub-micron cross sections made by nanolithography. Here we demonstrate spin transfer torque effects using point-contact spin injection involving no lithography. In a continuous Co/Cu/Co trilayer, we have observed hysteretic reversal of sub-100 nm magnetic elements by spin injection through a metal tip both at low temperature and at room temperature. A small magnetic domain underneath the tip in the top Co layer can be manipulated to align parallel or anti-parallel to the bottom Co layer with a unique bias voltage. In an exchange-biased single ferromagnetic layer, we have observed a new form of STT effect which is the inverse effect of domain wall magnetoresistance effect rather than giant magnetoresistance effect. We further show that in granular solids, the STT effect that can be exploited to induce a large spin disorder when combined with a large magnetic field. As a result, we have obtained a spectacular MR effect in excess of 400%, the largest ever reported in any metallic systems.

Keywords: spin transfer torque, point contact, current-induced switching, magnetic granular solids

1. Introduction

In the past, to reverse a magnetization, an external magnetic field is always required, such as the information bits written on the hard disks in our computer. The newly discovered spin transfer (STT) effect [1-13] provides another mechanism to alter a magnetization, which can be switched or excited by a spin-polarized current. In the giant magnetoresistance (GMR) effect, an external magnetic field changes the magnetic configuration resulting with low resistance for parallel configuration and high resistance for anti-parallel configuration. In the STT effect, an electric current affects the magnetic configuration without using a magnetic field. Consider the simplest case of a single electron with an arbitrary spin scattered by a single magnetic layer with magnetization pointing up. The magnetic layer works as a spin filter for the electron. After

scattering, the electron has only two possibilities: transmitted with spin up or scattered back with spin down. The horizontal component of spin has been transfer to the single magnetic layer in the form of the spin transfer torque. To observe the effect of this torque, a trilayer is often used. Indeed, the STT effect is the inverse effect of the GMR effect in the trilayer structure and both effects can be observed in the same trilayer structure.

In the trilayer, two magnetic layers are separated by a non-magnetic layer. The thicker magnetic layer (FM_{thick}) serves as the fixed layer while the thinner layer (FM_{thin}) with a smaller moment is the free layer. When electrons flow from the FM_{thick} to the FM_{thin} , they are polarized by the FM_{thick} and, when they reach the FM_{thin} , they tend to align the FM_{thin} in the same direction as that of FM_{thick} , thus parallel configuration is favored. When the current is reversed with electrons flowing from the FM_{thin} to the FM_{thick} , they are polarized by the FM_{thin} and then exert a torque on the FM_{thick} , but this toque is too small to have any effect on the FM_{thick} . Instead, some electron are scattered back by the FM_{thick} and their spins are in the opposite direction of the FM_{thick} . These electrons will align the FM_{thin} in the opposite direction of the FM_{thick} , thus anti-parallel configuration is favored. So parallel configuration is favored for one polarity of current and anti-parallel configuration is favored for the opposite. As a result, the magnetic configuration of the trilayer structure is asymmetric, depending on the polarity of the current. If a high magnetic field is applied, the free layer is preferentially aligned and precesses about the magnetic field as described by the Landan-Lifshitz equation. In reality, damping, as described by the Gilbert damping term, is inevitable and its effect is to align the magnetization to the field direction. The spin transfer torque introduces a third term and with appropriate polarity of current and sufficient current density, the spin torque term can cancel the damping term. Then the magnetization precesses about the field and works as a microwave generator.

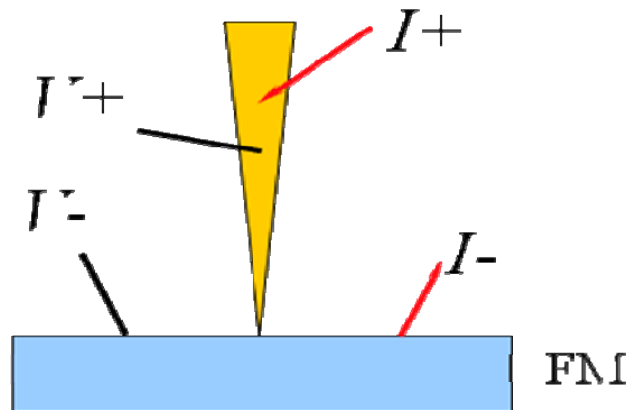


Figure 1 Schematic setup of a point-contact spin injection.

The current density required for the STT effect is rather high (e.g. $10^8 A/cm^2$). This is often achieved using a nano-pillar made by lithography with a cross section around 100 nm. We use a different method of point-contact spin injection to achieve the high current density required for the STT effect. A point contact is formed when a sharp tip is in contact with another material. The resistance (V/I) and differential resistance (dV/dI) are measured by a four-probe lock-in technique, as

shown in Figure 1. The contact size can be less than 10 nm, which can be determined from the contact resistance R_C . In the ballistic regime, R_C is Sharvin resistance [14] of $4\rho l/3\pi a^2$, with ρ the resistivity, l the electronic mean free path, and a the contact size. With a total current of only a few mAs, the current density can be as high as 10^9A/cm^2 , more than sufficient for the STT effect. In the following, we will describe the STT effects in three different systems studied by point-contact spin injection.

2. Current-induced switching effect in a continuous magnetic trilayer

The first system is a magnetic trilayer [15]. As shown in the inset of Figure 2, the essential structure is the Co(5.3 nm)/Cu(6.3 nm)/Co(180 nm) trilayer structure. The top Au(3 nm) layer is for protective purpose and the bottom superconducting Nb(350 nm) layer is for concentrating the current at 4.2 K when the Nb layer is superconducting. The resistance of one of the point contacts as a function of bias current at 4.2 K is shown in Figure 2 (red) using the top scale. The resistance basically falls onto two curves, high resistance and low resistance, with a hysteretic loop around zero current. Using a low current of 0.1 mA, which causes no STT effect, we measured the magnetoresistance (MR) of the same contact shown in blue using the bottom horizontal scale. The high resistance with anti-parallel configuration and low resistance with parallel configuration are exactly the same as the high and low resistance of the current-induced switching. This confirms that the magnetic configuration is switched by the spin-polarized current, thus resulting in the high and low resistance.

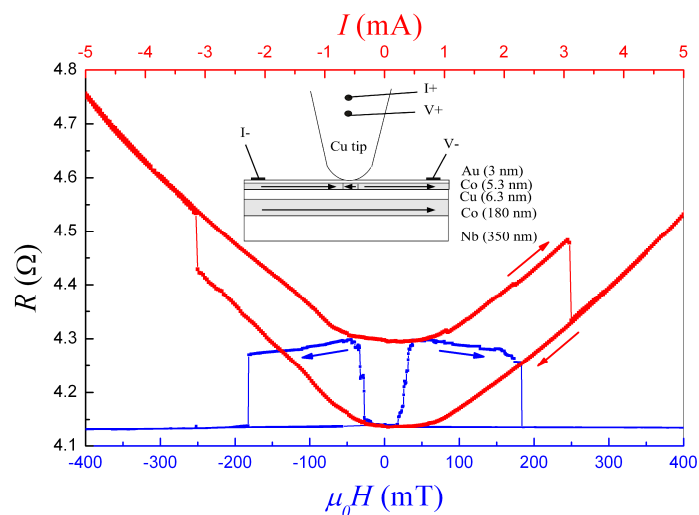


Figure 2 Resistance of one point contact as a function of current (red, top scale) and field (blue, bottom scale). Inset is the schematic of the experiment and sample structure.

We have observed switching effect for different contacts with various contact resistances. As shown in Figure 3(a-d), the switching current varies by one order of magnitude depending on the contact resistance. However, they can be correlated

by plotting them as a function of $1/R$, as shown in Figure 3(e), the positive and negative switching currents follow two lines. The linear dependence of $I_c = V_c/R_c$ indicates that there is a unique switching voltage V_c , which is independent of the contact resistance. From the results shown in Fig. 3(e), we obtain the values for the switching voltages as $V_c^+ = +10.7$ mV and $V_c^- = -12.3$ mV. We can also determine the switching current density from the switching voltage. Since $V_c = I_c R_c$, where I_c is $j_c \pi a^2$ with a the contact size and R_c is Sharvin resistance $4\rho l/3\pi a^2$ in ballistic regime, $V_c = j_c \pi a^2 \cdot 4\rho l/3\pi a^2 = 4j_c \rho l/3$ is only related to j_c because ρl is a constant for most of the metals. The unique switching voltage indicates a unique the switching current density and the values are: $j_c^+ = +(5.0 \pm 1.4) \times 10^8$ A/cm² and $j_c^- = -(6.0 \pm 1.3) \times 10^8$ A/cm².

It should be noted that the current-driven magnetic states are bi-stable at zero bias current. This is a prerequisite for information storage purposes. The well-defined switching voltages V_c^+ and V_c^- regardless of contact resistances have important technological implications. During the writing of a medium using a spin-polarized current, only a voltage pulse with amplitude exceeding V_c^+ or V_c^- needs to be applied across the contact to switch the magnetization of the bit underneath the tip. The values of V_c^\pm are relevant only to the thickness parameters of the multilayers and independent of the contact resistances.

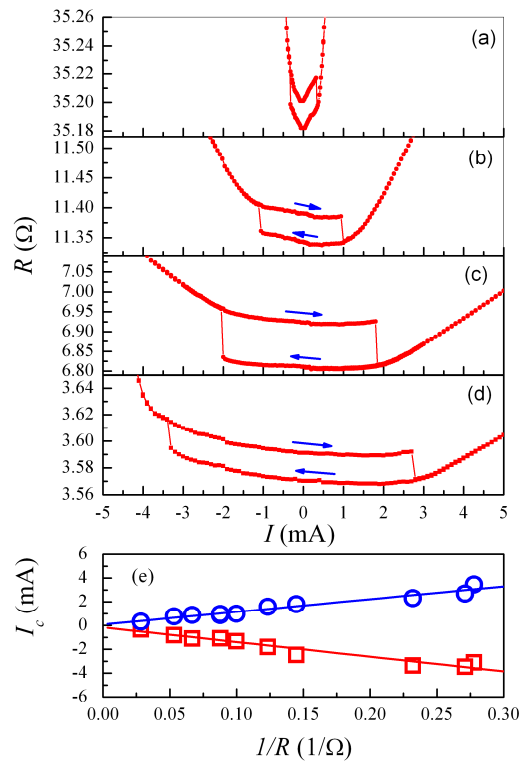


Figure 3 (a-d) Switching loops for various contact with decreasing contact resistance, and (e) the switching current as a function of $1/R_c$. Arrows indicate the sweeping direction of current.

3. Hysteretic switching in a single exchange-biased ferromagnetic layer

The second system studied by point-contact spin injection is for a Cu tip in contact with a single exchange-biased ferromagnetic layer in the form of 400 nm Co layer covered with a thin CoO layer [16]. The Co layer was made by magnetron sputtering and the CoO layer was formed by natural oxidation. The sample was cooled down in a field of 5T and the point contact was made at 4.2 K. Since there is only one single layer, we anticipate no effect. In contrast, we have observed hysteretic switching on both differential resistance (black) and resistance (red) shown in Figure 4(a). Different switching loops have been observed for various contact resistance. Depending on the contact resistance, the switching current can vary several times, but they all share a common current density, as shown in the inset of Figure 4(a).

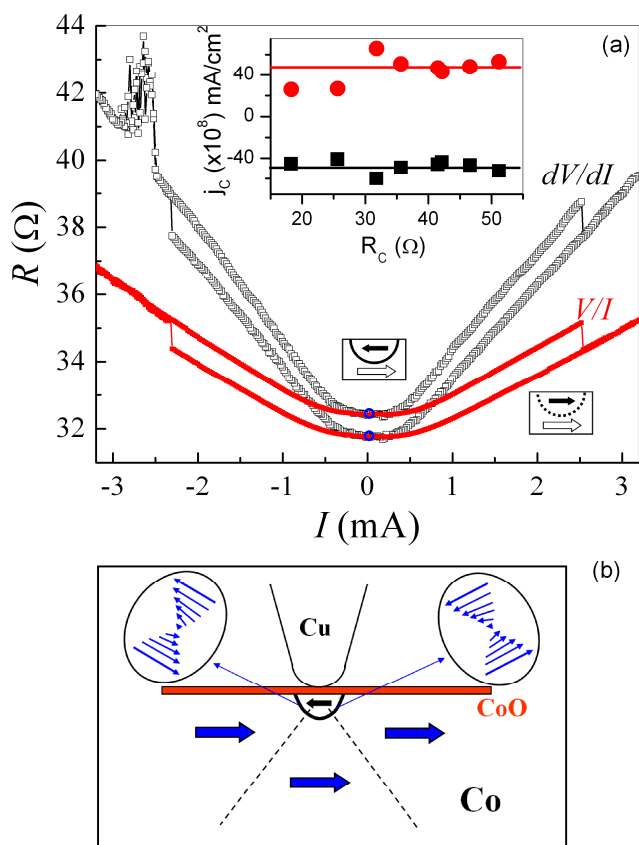


Figure 4 (a) Resistance (V/I) and differential resistance (dV/dI) of one Cu/CoO-Co point contact as a function of current, and (b) schematic domain structure near the point contact.

To find the physical origin of the switching effect, we further measured the MR using a small current of 0.1 mA, as shown in Figure 5. When the field is small (Figure 5(a)), the resistance has two resistance states: high (point d) and low (point c),

which are exactly the same as the high and low resistance states as current induced switching indicated by the blue dots in Figure 4(a). This suggests that there are two magnetic entities in the contact region and the resistance change induced by current is indeed due to a non-collinear magnetic structure in the contact region, as indicated by the spin structure in Figure 5(a). When a small field is applied, only the open arrow switches at points *b* and *c*, resulting in anti-parallel and parallel configurations for high and low resistance states. When a large field is applied, the solid arrow switches at *a* and *e*, showing an interesting curve with rich features as shown in Figure 5(b) where the spin configuration is indicated for each state. These data imply that there are two magnetic moments in the contact region and one behaves as the single layer, and the other has a much larger coercivity and it is exchange-biased as illustrated by Figure 5(c).

The evidence shows that there is a nano-domain, which is exchange-biased by the thin CoO layer, sitting on top of the single layer. Between the nano-domain and the Co layer, there is a domain wall, as illustrated in Figure 4(b). The current-induced switching effect observed here in a single layer is the inverse effect of domain wall MR, not the GMR effect as that in the multilayers [4-6, 15].

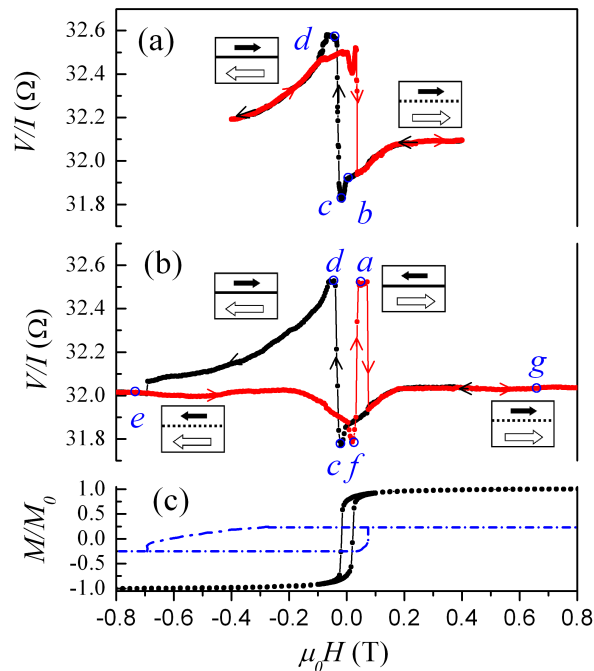


Figure 5 Magnetoresistance of the contact in Figure 4 using a current of 0.1 mA: (a) for field range (± 0.4 T), (b) field range (± 0.8 T), and (c) Magnetization (black data) and schematic loop of top (dashed curve). The arrows indicate the magnetic configurations.

We have studied the STT effect in a single layer under various magnetic fields up to 9 T, as shown in Figure 6. When the field is small, the switching loop does not change much. At a field about 0.5 Tesla, the loop collapses to the negative side and results in a step in the resistance, as shown in Figure 6(a). At higher fields, the step on the resistance shifts to more negative current (Figure 6(b)) and in the differential resistance the steps appear as spikes (Figure 6(c)).

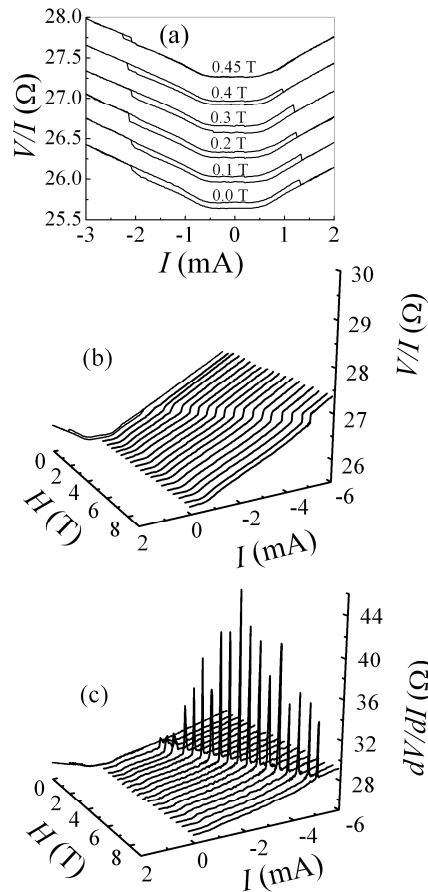


Figure 6 Field dependence of resistance V/I in the field range of (a) 0 to 0.5 T, (b) 0 T to 9 T and (c) differential resistance dV/dI from 0 T to 9 T.

The spikes have been previously attributed to spin wave or precession [3]. To further understand this feature, we plot the position of these spikes and the switching currents for the loops together, as shown in Figure 7(a). There are two switching currents at low fields but only one spike at high fields. For both the spikes at high fields and the switching at low fields, the critical currents follow the same linear dependence. This indicates that the spikes and the switching loops are likely due to the same physical origin. To further illustrate this scheme, we plot all the static resistance together, as shown in Figure 7(b). Solid line is the switching loop at low field and dash lines are the resistance steps at high fields. For both the resistance steps at high fields and switching loops at low fields, the resistance is basically switching

between two resistance states, parallel state or anti-parallel state. So the spike is actually an indication of non-hysteretic switching at high fields. These results show that even in a large field of 9 Tesla, the small domain can still be switched by the spin-polarized current of only 5 mA, vividly showing that large magnetic field is no match for the prowess of the spin transfer torque.

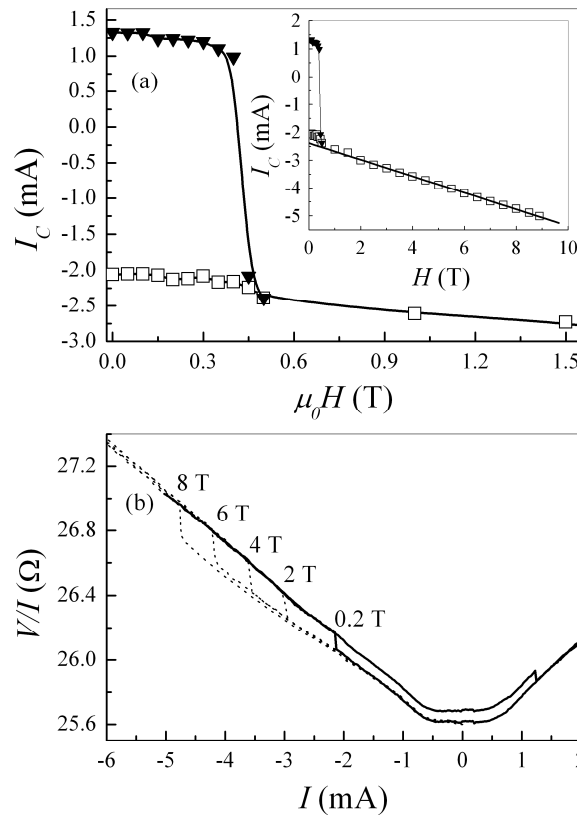


Figure 7 (a) Switching currents and spikes from 0 to 1.6 T, inset from 0 to 9.0 T, and (b) resistance in fields of 0.2 T, 2 T, 4 T, 6 T, 8 T.

4. Large magnetoresistance induced by spin transfer torque in magnetic granular solids

The last system that we will describe here is the STT effect in magnetic granular solids [17]. In addition to multilayers, GMR effect has also been observed in magnetic granular solids [18, 19]. Magnetic granular solids are formed by embedding nanometer scale magnetic granules such as Co into a non-magnetic medium such as Ag. At zero field, the magnetizations of granules are random showing zero net magnetization, but the resistance is maximum. When an external field aligns the magnetizations of the granules, the resistance is lowest but the magnetization is maximum. This

is the GMR effect in granular solids, different from that in trilayers where anti-parallel state gives the maximum resistance.

Since the STT effect is the inverse effect of the GMR effect, one should readily anticipate the STT effect in magnetic granular solids. However, as we'll see next, the STT effect in granular solids is even richer than just the inverse effect of GMR effect.

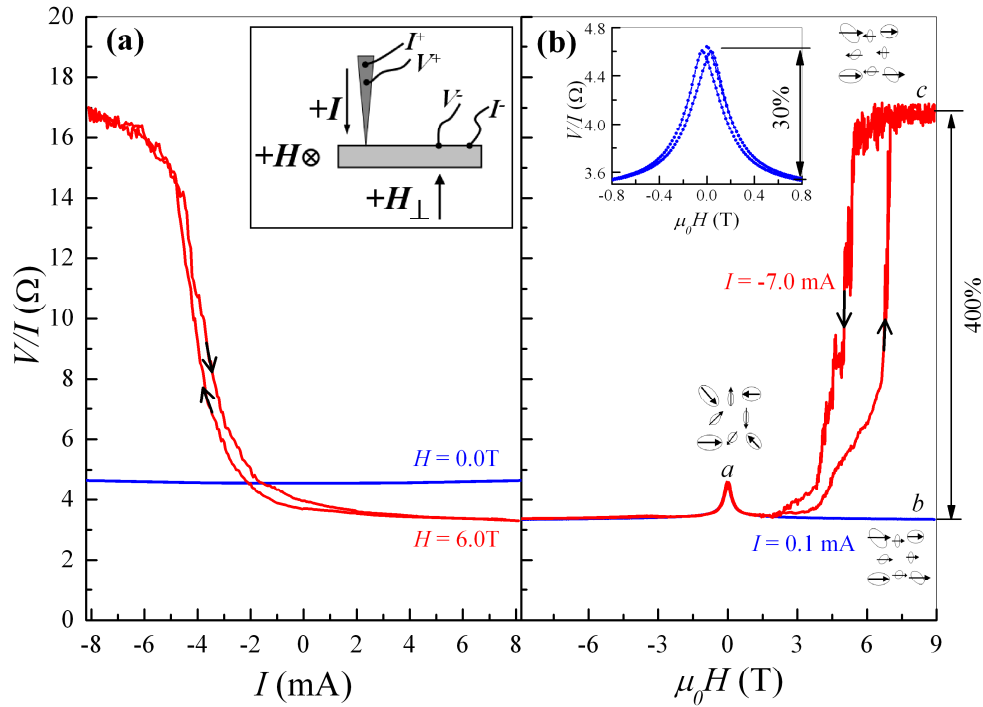


Figure 8 (a) Resistance versus current in 0 T and 6 T of granular $\text{Ag}_{82}\text{Co}_{18}$, inset shows schematics of point contact measurement, (b) magnetoresistance (MR) of 30% using currents 0.1 mA and 400% MR at -7 mA, and the schematic spin structures at *a*, *b*, and *c*; the inset shows MR in small field.

After a point contact is established on the granular solids, it shows the expected GMR of about 30%, as shown in the inset of Figure 8(b). Then we sweep the current, surprisingly there is no STT effect (Figure 8 (a) blue curve) even though there is large GMR effect. This is distinctively different from that in multilayer where both the STT effect and the GMR effect appear in the same structure. However, when we repeat the measurements with an in-plane magnetic field of 6 T, the resistance changes by a factor of 5, or 400% of GMR, as shown by the red curve in Figure 8(a). The same drastic change of resistance is confirmed by the MR measurement using a large current. The blue curve in Figure 8(b) is the MR

measured at 0.1 mA, which causes no STT effect. When the current is -7mA, the resistance changes 5 times (Figure 8(b) red curve), exactly the same as in the current sweeping.

At zero field, the granules have random magnetizations, thus the current is unpolarized. For an unpolarized current, there is no STT effect. When the granules are aligned by a large magnetic field, the resistance is low but the current is polarized. When the current density is sufficiently large, some of the small granules will be switched by the STT effect, forming an anti-ferromagnetic-like spin structure. This spin structure exhibits a much larger resistance than the random spin structure, causing the MR of 400%. This anti-ferromagnetic-like spin structure in granular solids cannot be achieved by any other means except the spin torque.

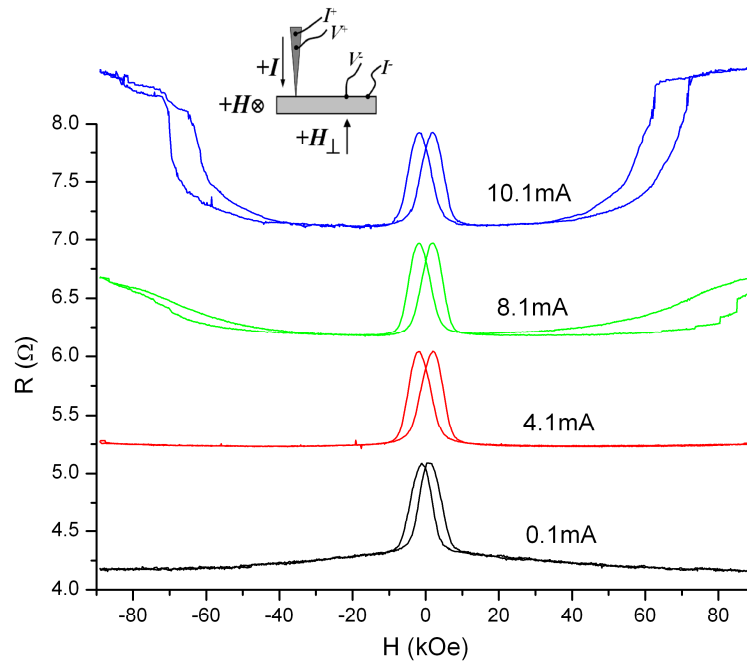


Figure 9 Magnetoresistance with various current for field perpendicular to the sample.

As shown in Figure 8, the STT effect seems to occur at one polarity of current or field. The asymmetry change to the opposite side when current or field is switched its polarity. Closer examination of the data shows that both sides have the effect with one side much larger than the other. We ascribe this asymmetry to the Oersted field generated by the current through the structure. As shown in the inset of Figure 8, the Oersted field of the order of 1 T in the vicinity of the point contact is added to, or subtracted from the applied magnetic field depending on the direction of the in-plane H and the locations of the electrical contacts on the sample. Indeed, as demonstrated in Figure 9, under a perpendicular H_{\perp} , the STT effect occurs symmetrically on both sides.

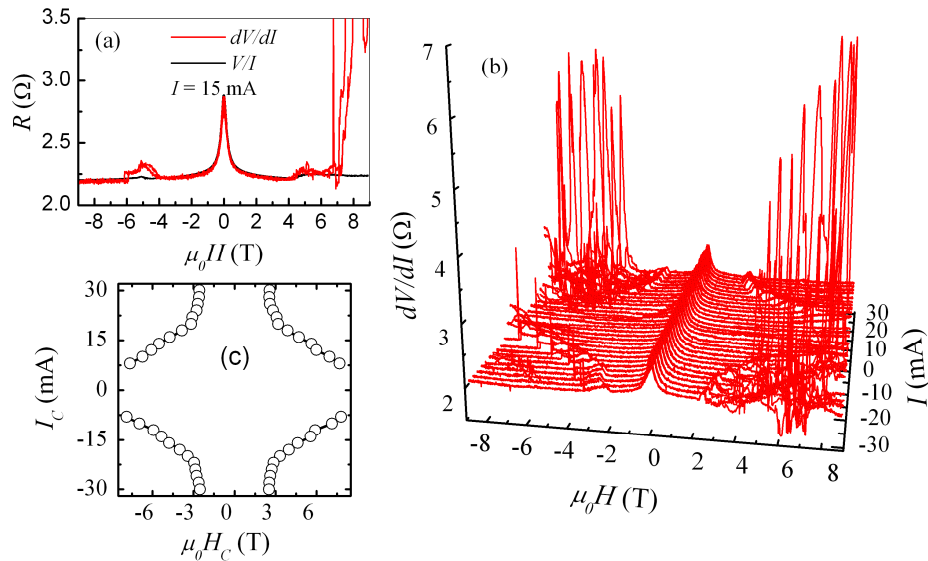


Figure 10 (a) Resistance (V/I) and differential resistance (dV/dI) of one point contact at $I = 15$ mA at 160 K, (b) differential resistance (dV/dI) for currents from -30 mA to 30 mA in fields from -9 T to 9 T at 160 K, and (c) critical currents at various fields.

At higher temperature such as 160 K, we haven't been able to observe the large resistance change. As shown in Figure 10(a), the resistance (V/I , black curve) shows only a small step. However, the more sensitive differential resistance (dV/dI , red curve) shows that the STT effect occurs symmetric with in-plane field and current. The differential resistance at various currents and in-plane fields are plotted in Figure 10(b) and critical currents extracted from this graph are plotted in Figure 10(c). No effect is observed at small fields in granular solids, which is distinctively different from that in multilayers or single layers, where current-induced switching is observed in small fields while non-hysteretic switching or spin wave is observed in high fields.

REFERENCES

- [1] J. Slonczewski, J. Magn. Magn. Magn. **159**, L1 (1996).
- [2] L. Berger, Phys. Rev. B **54**, 9353 (1996).

- [3] M. Tsoi, A. G. M. Jansen, J. Bass, W. C. Chiang, M. Seck, V. Tsoi, and P. Wyder, *Phys. Rev. Lett.* **80**, 4281 (1998).
- [4] E. B. Myers, D. C. Ralph, J. A. Katine, R. N. Louie, and R. A. Buhrman, *Science* **285**, 867 (1999).
- [5] J. A. Katine, F. J. Albert, R. A. Buhrman, E. B. Myers, and D. C. Ralph, *Phys. Rev. Lett.* **84**, 3149 (2000).
- [6] J. Z. Sun, D. J. Monsma, D. W. Abraham, M. J. Rooks, and R. H. Koch, *Appl. Phys. Lett.* **81**, 2202 (2002).
- [7] S. Zhang, P. M. Levy, and A. Fert, *Phys. Rev. Lett.* **88**, 236601 (2002).
- [8] F. B. Mancoff and S. E. Russek, *IEEE Trans Magn.* **38**, 2853 (2002).
- [9] Xavier Waintal, Edward B. Myers, Piet W. Brouwer, and D. C. Ralph, *Phys. Rev. B* **62**, 12317 (2000).
- [10] M. D. Stiles and A. Zangwill, *Phys. Rev. B* **66**, 014407 (2002).
- [11] D. C. Ralph and M. D Stiles, *J. Magn. Magn. Mater* **320**, 1190 (2008).
- [12] E. B. Myers, F. J. Albert, J. C. Sankey, E. Bonet, R. A. Buhrman, and D. C. Ralph, *Phys. Rev. Lett.* **89**, 196801 (2002).
- [13] F. J. Albert, N. C. Emley, E. B. Myers, D. C. Ralph, and R. A. Buhrman, *Phys. Rev. Lett.* **89**, 226802 (2002).
- [14] Yu. V. Sharvin, *JETP, (U.S.S.R.)* **48**, 984-985(1965)[*Sov. Phys.-JETP* **21**, 655 (1965)].
- [15] T. Y. Chen, Y. Ji, and C. L. Chien, *Appl. Phys. Lett.* **84**, 0380 (2004).
- [16] T. Y. Chen, Y. Ji, C. L. Chien, and M. D. Stiles, *Phys. Rev. Lett.* **93**, 026601 (2004).
- [17] T. Y. Chen, S. X. Huang, C. L. Chien and M. D. Stiles, *Phys. Rev. Lett.* **96**, 207203(2006).
- [18] Berkowitz, A. P. Young, J. R. Mitchell, S. Zhang, M. J. Carey, F. E. Spada, F. T. Parker, A. Hutten, and G. Thomas, *Phys. Rev. Lett.* **68**, 3745 (1992).
- [19] J. Q. Xiao, J. S. Jiang, and C. L. Chien, *Phys. Rev. Lett.* **68**, 3749 (1992).